Measurement of the Rate Coefficient for the Reaction of OH with BrO

Mary K. Gilles,*,† David C. McCabe,†,‡ James B. Burkholder, and A. R. Ravishankara†,‡

Aeronomy Laboratory, National Oceanic and Atmospheric Administration, 325 Broadway, Boulder, Colorado 80305-3328, USA

Received: October 26, 2000; In Final Form: March 28, 2001

We report the rate coefficient for the reaction OH + BrO → Products (1) at 298 K to be $k_1(298\ \mathrm{K}) = (4.5 \pm 1.8) \times 10^{-11}$ cm^3 molecule^{-1} s^{-1}. Reaction 1 was studied in an excess of BrO, generated in a flow tube, and measured via its UV−vis absorption. OH, produced by laser photolysis, was monitored by laser-induced fluorescence. Quoted uncertainties include estimated uncertainties in the BrO concentration and that due to the unavoidable concurrent reaction of OH with Br_2. Our measured value of k_1 is compared with that previously reported by Bogan et al.[1]

Introduction

Halogen oxides are important reactive intermediates in catalytic ozone destruction cycles in the stratosphere; examples include a reaction cycle such as

$$\mathrm{X} + \mathrm{O_3} \rightarrow \mathrm{XO} + \mathrm{O_2}$$

$$\mathrm{Y} + \mathrm{O_3} \rightarrow \mathrm{YO} + \mathrm{O_2}$$

$$\underline{\mathrm{XO} + \mathrm{YO} \rightarrow \rightarrow \mathrm{X} + \mathrm{Y} + \mathrm{O_2}}$$

$$2\ \mathrm{O_3} \rightarrow 3\ \mathrm{O_2}\ \mathrm{NET}$$

where X = H, OH, Cl, Br, or I and Y = NO, Cl, Br, and I. One such reaction involved in this type of cycle is that between OH and BrO.

$$\mathrm{BrO} + \mathrm{OH} \rightarrow \mathrm{Br} + \mathrm{HO_2} \quad (1a)$$

$$\rightarrow \mathrm{HBr} + \mathrm{O_2} \quad (1b)$$

This reaction can lead to ozone removal by bromine and is analogous to the ClO + OH reaction, which has been studied extensively over the past 20 years.[2] In addition to its participation in the ozone destruction cycle, reaction 1 is involved in partitioning stratospheric bromine between Br and BrO.

Currently, there is only a single measurement of k_1 at room temperature[1] and the product branching ratios remain unexplored. The primary reason for the lack of data on k_1 is the unavoidable experimental difficulty in determining k_1. In the single previous determination, BrO temporal profiles were measured by mass spectrometry in the presence of similar concentrations of OH. The measured concentration profiles were then fit to a reaction model to extract k_1. Aside from the difficulties with identifying all the reactions that may be contributing the temporal profiles of OH and BrO, there may be large uncertainties in the rate coefficients and initial conditions chosen in the model.

Chipperfield et al.[3] investigated the effect of this reaction, and in particular the possible HBr production in the stratosphere, on the composition of the stratosphere using a one-dimensional photochemical model. Using the only reported rate coefficient[1] for reaction 1, $k_1(300\ \mathrm{K}) = (7.5 \pm 4.2) \times 10^{-11}$ cm^3 molecule^{-1} s^{-1}, they concluded that a small, 1−2%, yield of HBr would account for the difference between modeled HBr and that measured by Nolt et al.[4] If the rate constant is smaller or larger, the branching ratio required to account for the observed HBr abundance will also change as will the possible effect of this reaction on the stratospheric composition.

In this work, we report measurements of k_1 at 298 K carried out in an excess of BrO where the OH temporal profiles were monitored by laser-induced fluorescence.

Experimental Section

Rate coefficients for reaction 1 were determined by monitoring OH temporal profiles in an excess of BrO. The apparatus used for measuring k_1 was essentially the same as the one used to study the reaction of OH with ClO[5] and is described in detail in previous publications.[6,7] Here, we will describe only the features that are essential for an understanding of the present study. Alterations to the apparatus and the experimental procedures were necessitated by the unavoidable difficulties in producing BrO in the absence of Br_2, which also reacts rapidly with OH

$$\mathrm{OH} + \mathrm{Br_2} \rightarrow \mathrm{HOBr} + \mathrm{Br}$$

$$k_2(298\ \mathrm{K}) = (4.3 \pm 0.7) \times 10^{-11}\ \mathrm{cm^3\ molecule^{-1}\ s^{-1}} \quad (2)$$

and the limited range of BrO concentrations that could be used.

Because we could not generate BrO in the absence of Br_2, k_1 was obtained by first measuring the first-order rate coefficient for OH loss in the presence of Br_2, then converting a fraction of Br_2 into BrO and remeasuring the OH loss rate coefficient. Thus, the value of k_1 measured by us depends on the value of k_2. The data analysis is described in more detail in the next section.

BrO Production and Detection. Passing a dilute mixture of Br_2 in He through a microwave discharge in a sidearm of

* To whom correspondence should be addressed. NOAA, R/AL2, 325 Broadway, Boulder, CO 80305-3328, USA, E-mail: mgilles@al.noaa.gov.

† Affiliated with the Cooperative Institute for Research in Environmental Sciences, University of Colorado, Boulder CO 80309, USA.

‡ Affiliated with the Department of Chemistry and Biochemistry, University of Colorado, Boulder, CO 80309, USA.

10.1021/jp0039666 CCC: $20.00
Published on Web 05/10/2001

the flow tube produced Br atoms. The Br atoms reacted with ozone, which was added ~3 cm downstream, to produce BrO. In a previous study on BrO + IO,[6] several tests were done to check for the loss of BrO radicals on the surface. These included variations of the flow velocities (by a factor of 2), pressure (a factor of 2), and using a Teflon insert to minimize radical loss to the walls. Those experiments were done at pressures and experimental conditions similar to the present experiments. In the BrO + IO experiments, variation of the above-mentioned parameters did not influence the measured rate coefficient. In addition, the rate coefficient measured was in agreement with that measured subsequently by Bedjanian et al.[8] Hence, we do not believe that heterogeneous loss of radicals to the surface was important in these experiments. The pressure in the flow tube was < 5 Torr of He and linear flow velocities of (710−805) cm s^{-1} led to residence times in the flow tube and reaction cell of ~70 ms, minimizing BrO loss due to its self-reaction. The BrO concentration in the absorption cell was measured using a 30 W deuterium lamp, a 0.3 m spectrograph (with a 1200 groove mm^{-1} grating), and a cooled 1024 element diode array detector. The deuterium lamp beam propagated through the reaction cell in the direction of the gas flow, opposite to the direction of the photolysis laser, and perpendicular to the probe laser beam. The optical path length through the reaction cell was 53.5 cm. Spectra in the wavelength range of 312 to 365 nm were recorded with a resolution of 0.5 nm (fwhm). This resolution matched that reported for the differential absorption cross section for the (7,0) band of BrO, 1.44×10^{-17} cm^2 $molecule^{-1}$.[6] Using the differential absorption signal minimized the error in the measured BrO concentration due to fluctuations in the deuterium lamp intensity.

The BrO concentration was determined from two diode array measurements of the transmitted light intensity, one with BrO, (I_{BrO}), and one without (I_0). For the I_{BrO} measurement, the mixture flowing through the reaction cell contains BrO, Br_2, O_3, and H_2O. The first three molecules absorb in the chosen wavelength range. I_0 was recorded after turning the microwave discharge off; under this condition, the absorption cell contained Br_2, O_3, and H_2O. The BrO concentrations were calculated by assuming optically thin conditions and using the measured value of absorbance, $A = [BrO]\sigma l$, where σ is the differential absorption cross section and l is the path length. Typical BrO differential absorbances range from 1 to 5×10^{-3} corresponding to BrO concentrations of $(1.3-6.5) \times 10^{12}$ molecules cm^{-3}. Br_2 was not observed in the spectra because its absorbance between 312 and 365 nm would be $< 6 \times 10^{-5}$, given that the maximum absorption cross section[9] of Br_2 in this wavelength region is 1.68×10^{-19} cm^2 $molecule^{-1}$ and that Br_2 concentrations were $(1.2-6.9) \times 10^{12}$ molecules cm^{-3}.

The measured UV−vis absorbance yielded the column BrO abundance, and hence the average BrO concentrations along the length of the absorption cell. Because of the BrO self-reaction, a concentration gradient existed along the length of the reaction cell. About 85% of the BrO self-reaction produced Br atoms that subsequently reacted with ozone that was present in excess to regenerate BrO. Thus, the concentration gradient was smaller than what would be obtained in the absence of O_3, which converts Br back to BrO. Calculation of the BrO concentration in the reaction volume from the measured column abundance is discussed in detail elsewhere.[6] Because the intersection of the two laser beams was in the center of the BrO absorption cell, the agreement between the [BrO] modeled at this point, and the calculated column average were within 8%. The measured column average concentration was used in calculating k_1.

OH Production and Detection. OH was generated by the pulsed laser photolysis (248 nm) of O_3

$$O_3 + h\nu \rightarrow O(^1D) + O_2\,(^1\Delta) \quad (3a)$$

$$\rightarrow O(^3P) + O_2\,(^3\Sigma) \quad (3b)$$

which produces $O(^1D)$ that reacted[2] with H_2O to give OH

$$O(^1D) + H_2O \rightarrow 2\,OH \qquad k_4(298\ K) = 2.2 \times 10^{-10}\ cm^3\ molecule^{-1}\ s^{-1} \quad (4)$$

The LIF signal from OH was measured as a function of time by varying the delay between the photolysis and probe lasers from 0 to 10 ms. The sensitivity for OH detection, as measured by a signal-to-noise ratio of one, was $\sim 7 \times 10^8$ radicals cm^{-3} for averaging 100 laser pulses. The concentration of H_2O in the cell, $(3-20) \times 10^{13}$ molecules cm^{-3}, was calculated from its vapor pressure at the ambient temperature, measured gas flow rate through the bubbler containing water, other gas flow rates, and cell pressure. We worked with initial concentrations of OH, $[OH]_0$, $< 2 \times 10^{11}$ molecules cm^{-3} to ensure pseudo-first-order conditions in OH even while using low BrO concentrations. We obtained low $[OH]_0$ by using very low laser fluence, <0.01 mJ cm^{-2} $pulse^{-1}$, with the abundance of ozone required to rapidly convert Br back to BrO. These low laser fluences could not be measured accurately. Therefore, we first calibrated the LIF signal from OH at the beginning of each experiment using low ozone concentrations (8×10^{13} molecules cm^{-3}) and measurable photolysis laser fluence (0.03 mJ $pulse^{-1}$ cm^{-2}). For this calibration, $[OH]_0$ was calculated from $[O_3]_0$, the photolysis laser fluence, the O_3 absorption cross section at 248 nm (1.17×10^{-17} cm^2 $molecule^{-1}$), the quantum yield for $O(^1D)$ formation (0.9), and the yield of two OH for each $O(^1D)$ formed.[2] In subsequent kinetics experiments, the initial OH concentrations were obtained from the measured OH signal and the calibration factor determined using the higher fluence; $[OH]_0$ ranged from $(0.4-1.9) \times 10^{11}$ molecules cm^{-3}.

Under our experimental conditions, a small fraction of $O(^1D)$ could react with either Br_2,[10] BrO,[2] or O_3.[2] If $O(^1D)$ reacted with O_3 the resulting $O(^3P)$ could further react with Br_2 or BrO and, thus, influence [BrO]

$$O(^3P) + Br_2 \rightarrow BrO + Br \qquad k_5(298\ K) = 2 \times 10^{-11}\ cm^3\ molecule^{-1}\ s^{-1} \quad (5)$$

$$O(^3P) + BrO \rightarrow Br + O_2 \qquad k_6(298\ K) = 4.1 \times 10^{-11}\ cm^3\ molecule^{-1}\ s^{-1} \quad (6)$$

Photolysis of ozone to produce O atoms could increase [BrO] by as much as 7% at the highest laser fluence and lowest [BrO] used. As seen in Table 1, increasing $[H_2O]$ by a factor of 5, thereby decreasing $[O(^3P)]$, did not affect the measured value of k_1. Although a small amount of BrO is produced by $O(^3P)$ reactions, given the relatively large uncertainty in our measured value of k_1, it is unlikely to effect the quoted results.

Materials. He (UHP, 99.997%) was flowed through a molecular sieve trap held at 77 K to remove condensable impurities. Ozone was prepared by passing O_2 (UHP, 99.99%) through a commercial ozonizer and stored on a silica gel trap at 195 K. Ozone was eluted from this trap by flowing a small

TABLE 1: Experimental Conditions for Various Sets of Data Points[a]

Torr	[BrO]	$[Br_2]_0$	$[O_3]$	$[BrO]/[OH]_0$	$[BrO]/[Br_2]_0$	$[H_2O]$	$[OH]_0$[b]	v	symbol[c]
4.2	1.25−3.10	1.2−6.9	0.7−4.3	24−60	0.4−1	3	4−9	780	■
4.8	2.58−5.57	1.9−5.6	1−1.8	28−71	0.7−1.2	4	6−11	780	▼
4.8	5.00−6.46	5.0−6.6	0.6−1.9	48−68	0.9−1.0	3	9−11	805	○
3.6	2.75−4.37	2.8−4.6	0.6−1.8	14−47	0.9−1.0	4	8−19	710	◆
4.3	2.08−4.41	2.2−5.8	0.7−1.0	14−37	0.7−1.1	3	8−14	760	▽
4.8	4.62−6.97	5.8−6.8	2.2	16−47	0.1−1.2	20	12−18	725	□

[a] Units are [BrO], 10^{12} molecules cm^{-3}; $[Br_2]_0$, 10^{12} molecules cm^{-3}; $[O_3]$, 10^{14} molecules cm^{-3}; $[H_2O]$, 10^{13} molecules cm^{-3}; [OH], 10^{10} molecules cm^{-3}; linear velocity, v: cm s^{-1}. [b] This is from the calculated maximum initial $O(^1D)$ concentration. The $[OH]_0$ is lower than this due to the reactive loss of $O(^1D)$ as described in the text. $[BrO]/[Br_2]$ is the ratio of BrO concentration measured by absorbance to the initial Br_2 concentration. If all Br_2 were converted into BrO this ratio would be 2. [c] These symbols are used in Figure 2.

amount of He through it. In most experiments, $[O_3]_0$ ($\sim 1 \times 10^{14}$ molecules cm^{-3}) was measured in a 50 cm cell prior to entering the flow tube where it was further diluted with He (dilution factors were from 2 to 10) to obtain the needed concentration. The ozone concentration in the LIF reaction cell was calculated from the measured $[O_3]_0$, the dilution factor, and the pressure difference between the two cells. Br_2 (99.99+%) was stored in a bubbler maintained at 195 K. The flow of He through this bubbler was varied to change the Br_2 concentration in the reaction cell. Distilled water was stored in a room-temperature bubbler and varying the flow of He through the bubbler regulated its concentration in the reaction cell.

Results and Discussion

The measured OH temporal profiles were defined by the following set of reactions

$$OH \rightarrow \text{loss} \tag{7}$$

$$OH + O_3 \rightarrow HO_2 + O_2 \tag{8}$$

$$OH + BrO \rightarrow \text{Products} \tag{1}$$

$$OH + Br_2 \rightarrow HOBr + Br \tag{2}$$

Reaction 7 represents the first-order loss of OH due to reaction with impurities and flow out of the detection region. For each set of experimental parameters (i.e., initial concentrations, laser fluences and flow conditions) three separate OH temporal profiles were measured. The first OH temporal profile, I, was measured in the absence of Br_2 and BrO and the OH loss rate coefficient was given by

$$\frac{\ln\{[OH]_t^I/[OH]_{t=0}^I\}}{t} = -(k_7 + k_8[O_3]) = -k_I' \qquad \text{(I)}$$

where $[OH]_t^I$ is the OH concentration at time t. k_I' was obtained as the slope from a weighted linear least-squares fit of $\ln\{[OH]_t^I\}$ vs t to a straight line.

The second OH profile, II, was measured with Br_2 added to the gas flow. The OH loss rate coefficient in this case was given by

$$\frac{\ln\{[OH]_t^{II}/[OH]_{t=0}^{II}\}}{t} = -(k_2[Br_2]_0 + k_7 + k_8[O_3]) = -k_{II}' \tag{II}$$

The difference between the first-order loss rate coefficients from the two OH temporal profiles, $k_{II}'-k_I'$, yielded k_2', where $k_2' = k_2[Br_2]_0$. This value of k_2' was combined with our value of k_2 to determine $[Br_2]_0$. In this analysis we assume that OH loss from reactions 7 and 8 was not affected by the addition of Br_2. This was consistent with our calculations of ozone loss during BrO production as well as the observed invariance (within 10%) in the ozone concentration as measured by UV absorption.

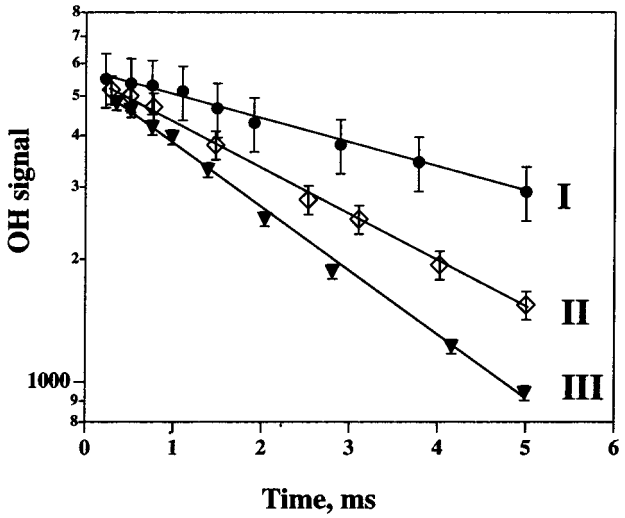

Figure 1. Examples of the three temporal profiles measured to derive k_1. The OH temporal profile I (filled circles) in the presence of O_3 (7×10^{13} molecules cm^{-3}), was measured in the absence of Br_2 and BrO; II (open diamonds) was measured with Br_2 ($[Br_2]_0 = 2.80 \times 10^{12}$ molecules cm^{-3}) added through the microwave discharge but with the discharge off; III (filled triangles) was measured with the microwave discharge on where BrO (2.75×10^{12} molecules cm^{-3}) was produced. The lines are the weighted least-squares fits to the data.

The third OH temporal profile, III, was measured after turning on the microwave discharge and producing BrO. The OH loss rate coefficient, k_{III}', was given by

$$\frac{\ln\{[OH]_t^{III}/[OH]_{t=0}^{III}\}}{t} = -(k_1[BrO] + k_2[Br_2]_f + k_7 + k_8[O_3]) = -k_{III}' \tag{III}$$

where $[Br_2]_f$, was related to the initial Br_2 concentration by

$$[Br_2]_f = [Br_2]_0 - [BrO]/2 \tag{IV}$$

Hence, the slope of a plot of the difference between the first-order rate coefficients, $k_{III}'- k_{II}'$, vs [BrO], yielded a slope of $(k_1 - k_2/2)$, from which k_1 was determined using previously measured values of k_2. This assumes that Br is not lost in the $\sim$3 cm it travels in the flow tube prior to the introduction of ozone and that Br_2 is not lost to the reactor walls.

A representative set of OH temporal profiles is shown in Figure 1. Typical values of the first-order rate coefficients for loss of OH observed in these experiments were 280 s^{-1} for k_I', 300−800 s^{-1} for k_{II}', and 360 to 860 s^{-1} for k_{III}'. As shown in Figure 1, the first order loss rate coefficient nearly doubled when Br_2 was added to the reaction cell. Turning on the microwave discharge to produce BrO further increased the first-order OH

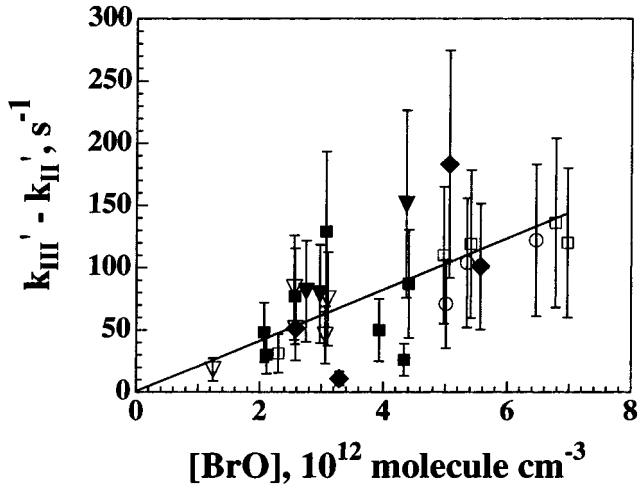

Figure 2. A plot of $k_{III}'-k_{II}'$ vs [BrO]. This plot yields a slope of $(k_1 - k_2/2) = (2.06 \pm 0.32) \times 10^{-11}$ cm^3 molecule^{-1} s^{-1}. Combining this quantity with a value of k_2(298 K) of 4.8×10^{-11} cm^3 molecule^{-1} s^{-1} yields a value for k_1(298 K) of $(4.5 \pm 1.8) \times 10^{-11}$ cm^3 molecule^{-1} s^{-1}. The uncertainty includes the estimated systematic errors (see text).

loss rate coefficient by 5 to 36%. The observed increase in the OH loss rate coefficient upon generation of BrO implies that $k_1 > k_2/2$.

Figure 2 shows a plot of $k_{III}'-k_{II}'$ vs BrO. The slope is $k_1 - k_2/2$ and the intercept should be zero. A nonweighted linear least-squares fit yielded an intercept which was zero within the uncertainty of the fit. Therefore, we fit the data with a fixed intercept of zero and obtained a slope of $(2.06 \pm 0.32) \times 10^{-11}$ cm^3 molecule^{-1} s^{-1}, as shown in Figure 2. This uncertainty represents 2σ precision of the unweighted fit. There are five experimental determinations of k_2(298 K) (all in units of 10^{-11} cm^3 molecule^{-1} s^{-1}) of 3.96,[11] 4.8,[12] 5.28,[13] 4.2,[14] and 3.4,[15] leading to an average value of $k_2(298\ \text{K}) = (4.3 \pm 0.7) \times 10^{-11}$ cm^3 molecule^{-1} s^{-1}. We prefer to use our recently measured value[12] of k_2(298 K) of $(4.8 \pm 0.7) \times 10^{-11}$ cm^3 molecule^{-1} s^{-1}, where the quoted uncertainty is the overall estimated error at the 95% confidence level. We prefer this value because it was measured as a prelude to measuring k_1 and was determined using the identical experimental apparatus. Using this value of k_2, we obtain $k_1(298\ \text{K}) = (4.5 \pm 0.7) \times 10^{-11}$ cm^3 molecule^{-1} s^{-1} from the measured value of $(k_1 - k_2/2)$, and the uncertainty in k_2.

We quote k_1 with a total uncertainty, at the 95% confidence level, to be $k_1(298\ \text{K}) = (4.5 \pm 1.8) \times 10^{-11}$ cm^3 molecule^{-1} s^{-1}. The overall uncertainty was obtained by adding the uncertainties in the fits of the temporal profiles in the presence of Br_2 and BrO (~3% each), the uncertainty in the BrO concentration from its absorption measurement and concentration gradient (16%), and the uncertainty in [BrO] due to photolytic production (7%) to the uncertainty in the value of k_1 noted above. Adding the fractional uncertainties, rather than assuming the uncertainties to be independent of one another and combining them in quadrature, yields the quoted maximum uncertainty of ~40%. Our experiment determines the quantity $(k_1 - k_2/2)$. Therefore, if k_2 were revised in future experiments, our value of $(k_1 - k_2/2)$ can be used to recalculate k_1 (298 K).

We employed the above method to determine k_1 because there are several important experimental difficulties. First, it is essentially impossible to produce and maintain significant concentrations of BrO in the absence Br_2. This is mostly because good precursors for BrO, such as OBrO and Br_2O, are highly unstable and also contain Br_2. Further, even if BrO were produced cleanly, it is not possible to maintain a constant concentration of BrO in the absence of Br_2 because it is rapidly produced via the self-reaction of BrO

$$\text{BrO} + \text{BrO} \rightarrow \text{Br}_2 + \text{O}_2 \qquad k_{9a}(298\ \text{K}) = 3.8 \times 10^{-13}\ \text{cm}^3\ \text{molecule}^{-1}\ \text{s}^{-1} \quad (9a)$$

$$\rightarrow 2\ \text{Br} + \text{O}_2 \qquad k_{9b}(298\ \text{K}) = 2.1 \times 10^{-12}\ \text{cm}^3\ \text{molecule}^{-1}\ \text{s}^{-1} \quad (9b)$$

Even if Br was recycled via reaction with ozone,[2] as in the current study, via the reaction

$$\text{Br} + \text{O}_3 \rightarrow \text{BrO} + \text{O}_2 \qquad k_{10}(298\ \text{K}) = 1.2 \times 10^{-12}\ \text{cm}^3\ \text{molecule}^{-1}\ \text{s}^{-1} \quad (10)$$

production of Br_2 cannot be suppressed completely. To add to this difficulty, the reaction of Br_2 with OH, reaction 2 is very rapid. This situation is to be contrasted with the case of ClO, which can be easily produced via reactions such as Cl + OClO and Cl + Cl_2O in either discharge flow tubes or pulsed photolysis systems. Futhermore, the rate coefficient for the reaction of OH with Cl_2

$$\text{OH} + \text{Cl}_2 \rightarrow \text{HOCl} + \text{Cl} \qquad k_{11}(298\ \text{K}) = 6 \times 10^{-14}\ \text{cm}^3\ \text{molecule}^{-1}\ \text{s}^{-1} \quad (11)$$

is nearly a thousand times slower[12] than k_2.

Because we used reaction 10 to produce BrO and needed a large ozone concentration, we could not vary the concentration of BrO over a wide range. Higher concentrations of BrO lead to higher concentrations of Br_2 and the efficiency of BrO production also decreased, which exacerbated this situation.

Bogan et al.[1] report a value of $k_1(300\ \text{K}) = (7.5 \pm 4.2) \times 10^{-11}$ cm^3 molecule^{-1} s^{-1}. They used a discharge flow tube equipped with mass spectrometric detection of OH, BrO, and Br_2. The $[\text{BrO}]_0/[\text{OH}]_0$ ranged from 0.4 to 1.2 in their experiments. OH was formed in a sidearm via the reaction

$$\text{F} + \text{H}_2\text{O} \rightarrow \text{OH} + \text{HF} \quad (12)$$

and BrO was formed in a separate sidearm by flowing a He/Br_2/O_2 mixture through a microwave discharge. The radical concentrations were determined by chemical titration. Recently, such BrO generation has been shown to produce other bromine oxide species such as OBrO,[16] whose reactivity with OH is unknown. Bogan et al. determined k_1 from the least-squares fit of the fractional consumption of BrO, $(1 - [\text{BrO}]_t/[\text{BrO}]_0)$, vs time to a reaction model consisting of a sequence of reactions. The reaction model contained a number of secondary reactions but the obtained value of k_1 was most sensitive to reactions 1, 2, 9, and the OH, BrO, and Br_2 concentrations. They quoted 2σ uncertainty from the precision of the fit and did not include any uncertainties in the reaction rate coefficients or concentrations. Nevertheless, given the large uncertainties in both of these experiments, largely due to the difficulty of this experiment, the two values of k_1 overlap with one another. We believe that our experiments are more accurate because they were carried out under pseudo-first-order conditions in OH and modeling of the temporal profiles was not required. Additionally, by measuring the difference between the two temporal profiles, we have reduced possible systematic uncertainties in our measurements.

Sumathi and Peyerimhoff predict that the HBr product from reaction 1 is unimportant below 2000 K.[17] This conclusion was

based upon their theoretical study showing a barrier height for HOOBr dissociation to HBr + O_2 lying several kcal mol^{-1} above the energy of the reactants. This result is analogous to their conclusion on the ClO + OH reaction, except that the barrier height for dissociation of HOOCl to HCl + O_2 was about 3 times larger. Although the theoretical calculations[17] predict HBr production to be an unimportant channel at atmospheric temperatures, HBr production cannot be ruled out. This is particularly true because HCl has been reported as a product of the OH + ClO reaction and the calculated barrier for the HBr production is smaller than that for HCl production. If the branching ratio for HBr formation in reaction 1 is a few percent, it will have a significant effect in the atmosphere. Our value for k_1 is lower than that used by Chipperfield et al.[3] in their 1D model. Therefore, to account for the difference between measured and calculated HBr levels in the stratosphere using our value of k_1 would require a larger branching ratio for HBr production in reaction 1.

The value of k_1 reported here is about a factor of 2 larger than that for the analogous ClO + OH reaction. By analogy with the rate coefficient for the similar reaction of ClO with OH, k_1 is expected to exhibit a small temperature dependence. Given the large uncertainties in the two experimental determinations of k_1 (298 K), it would be difficult to accurately determine $k_1(T)$. If a method can be found to monitor BrO temporal profiles at low concentrations and under good pseudo first-order conditions in OH, k_1 could be determined more accurately. Such a method would eliminate, or minimize, the experimental uncertainty due to reaction 2. Delmdahl and Gericke[18] recently reported the detection of BrO via two-photon LIF. Therefore, we made numerous attempts to detect BrO via two-photon LIF: these experiments were unsuccessful and are presented in the Appendix.

Appendix

Two Photon Laser-Induced Detection of BrO. Measuring k_1 by monitoring BrO temporal profiles in a large excess ([OH]/[BrO] at least > 10) of OH could yield a more accurate value. Under pseudo first-order conditions in BrO, the reaction of Br_2 with OH can be minimized more effectively. Therefore, we attempted to monitor BrO via two photon LIF as reported recently.[18]

For our measurements, the doubled output (15−20 mJ $pulse^{-1}$) from a Nd:YAG pumped dye laser was focused with quartz lenses of a variety of focal lengths and scanned over the range (350−354) nm. BrO was produced either by 248 nm photolysis of a mixture of O_3 ($\sim 3 \times 10^{16}$ molecules cm^{-3}) and CF_3Br ($\sim 1.5 \times 10^{16}$ molecules cm^{-3}) or by using reaction 10 in the flow tube. When using reaction 10, the concentration of BrO as monitored by UV/Visible absorption, ranged from $(1-7) \times 10^{12}$ molecules cm^{-3}. Both MgF_2 and Quartz lenses were used for focusing the fluorescence onto either a Hamamatsu R1459 (MgF_2 window, CsI photocathode, 115−200 nm) or a Hamamatsu R6836 (MgF_2 window, CsTe photocathode, 115−320 nm) photomultiplier tube. We attempted to collect broadband fluorescence from BrO using a 183 nm band-pass filter (47 nm fwhm). We were unable to observe any LIF signal that could be attributed to BrO, even though scattered laser light was minimal using the R1459 photomultiplier. Using the same system, we could detect ClO via two photon LIF by scanning the doubled laser dye output over the range of 340−344 nm and focusing the beam with a quartz lens. Spectra similar to those previously reported for ClO were readily observed.[19,20] We estimate our sensitivity for detection of ClO to be $(1-9) \times 10^{11}$ molecules cm^{-3} for a signal-to-noise ratio of 1 for 100 laser pulses, similar to previous reports. Hence, we are unable to confirm that the fluorescence signal observed by Delmdahl and Gericke[18] was that of BrO. However, we should note that Delmdahl and Gericke estimated that the BrO concentrations in their experiments could be as large as 2×10^{15} molecules cm^{-3}, several orders of magnitude larger than that used in our experiments. If such large BrO concentrations are necessary for 2 photon LIF detection, it is not advantageous to use this method to measure k_1. This is both because it will be difficult to operate under pseudo-first-order conditions in BrO and the influence of the BrO self-reaction.

Acknowledgment. This work was funded in part by the Upper Atmospheric Research Program of NASA. David McCabe acknowledges a NSF Graduate Research Fellowship.

References and Notes

(1) Bogan, D. J.; Thorn, R. P.; Nesbitt, F. L.; Stief, L. J. *J. Phys. Chem.* **1996**, *100*, 14 383.
(2) DeMore, W. B.; Sander, S. P.; Golden, D. M.; Hampson, R. F.; Kurylo, M. J.; Howard, C. J.; Ravishankara, A. R.; Kolb, C. E.; Molina, M. J. "Chemical Kinetics and Photochemical Data for Use in Stratospheric Modeling," Jet Propulsion Laboratory, 1997.
(3) Chipperfield, M. P.; Shallcross, D. E.; Lary, D. J. *Geophys. Res. Lett.* **1997**, *24*, 3025.
(4) Nolt, I. G.; Ade, P. A. R.; Alboni, F.; Carli, B.; Carlotti, M.; Cortesi, U.; Epifani, M.; Griffin, M. J.; Hamilton, P. A.; Lee, C.; Lepri, G.; Mencaraglia, F.; Murray, A. G.; Park, J. H.; Park, K.; Raspollini, P.; Ridolfi, M.; Vanek, M. D. *Geophys. Res. Lett.* **1997**, *24*, 281.
(5) Kegley-Owen, C.; Gilles, M. K.; Burkholder, J. B.; Ravishankara, A. R. *J. Chem. Phys. A.* **1999**, *103*, 5040.
(6) Gilles, M. K.; Turnipseed, A. A.; Burkholder, J. B.; Ravishankara, A. R.; Solomon, S. *J. Phys. Chem. A* **1997**, *101*, 5526.
(7) Vaghjiani, G. L.; Ravishankara, A. R. *J. Phys. Chem.* **1989**, *93*, 1948.
(8) Bedjanian, Y.; LeBras, G.; Poulet, G. *J. Phys. Chem. A* **1998**, *102*, 10 501.
(9) Maric, D.; Burrows, J. P.; Moortgat, G. K. *J. Photochem. Photobiol. A: Chem* **1994**, *83*, 179.
(10) Nicovich, J. M.; Wine, P. H. *Int. J. Chem. Kinet.* **1990**, *22*, 379.
(11) Bedjanian, Y.; LeBras, G.; Poulet, G. *Int. J. Chem. Kinet.* **1999**, *31*, 698.
(12) Gilles, M. K.; Burkholder, J. B.; Ravishankara, A. R. *Int. J. Chem. Kinet.* **1999**, *31*, 417.
(13) Loewenstein, L. M.; Anderson, J. G. *J. Phys. Chem.* **1984**, *88*, 6277.
(14) Poulet, G.; Laverdet, G.; LeBras, G. *Chem. Phys. Lett.* **1983**, *94*, 129.
(15) Boodaghians, R. B.; Hall, I. W.; Wayne, R. P. *J. Chem. Soc., Faraday Trans. 2* **1987**, *83*, 529.
(16) Knight, G.; Ravishankara, A. R.; Burkholder, J. B. *J. Phys. Chem. A* **2000**, *104*, 11 121.
(17) Sumathi, R.; Peyerimhoff, S. D. *Phys. Chem. Chem. Phys.* **1999**, *1*, 3973.
(18) Delmdahl, R. F.; Gericke, K.-H. *J. Chem. Phys.* **1998**, *109*, 2049.
(19) Matsumi, Y.; Shamsuddin, S. M.; Kawasaki, M. *J. Chem. Phys.* **1994**, *101*, 8262.
(20) Baumgärtel, S.; Gericke, K.-H. *Chem. Phys. Lett.* **1994**, *227*, 461.